

# Thermal Conductivity of $\text{CaSrFe}_2\text{O}_{6-\delta}$

Ebony Schultz<sup>1</sup>, Mandy Guinn<sup>1</sup>, Alexa D Azure<sup>2</sup> and Ram Krishna Hona<sup>1\*</sup>

<sup>1</sup>Environmental Science Department, United Tribes Technical College, Bismarck, USA

<sup>2</sup>Engineering Department, United Tribes Technical College, Bismarck, USA

Submission: December 22, 2023; Published: January 10, 2024

\*Corresponding author: Ram Krishna Hona, Environmental Science Department, United Tribes Technical College, Bismarck, USA

## Abstract

The thermal conductivity of  $\text{CaSrFe}_2\text{O}_{6-\delta}$ , an oxygen-deficient perovskite, is a critical parameter for understanding its thermal transport properties and potential applications in energy conversion and electronic devices. In this study, we present an investigation of the thermal conductivity of  $\text{CaSrFe}_2\text{O}_{6-\delta}$  at room temperature for its thermal insulation property study. Experimental measurement was conducted using a state-of-the-art thermal characterization technique, Thermtest thermal conductivity meter. The thermal conductivity of  $\text{CaSrFe}_2\text{O}_{6-\delta}$  was found to be 0.574W/m/K, exhibiting a notable thermal insulation property

**Keywords:** Thermal conductivity; Energy conversion; Thermoelectric devices; Energy storage; Catalysis

## Introduction

Perovskite oxides have garnered considerable attention in recent years due to their versatile properties, which make them promising candidates for a variety of technological applications, including thermoelectric devices [1], catalysis [2], and energy storage systems [3]. Among these oxides,  $\text{CaSrFe}_2\text{O}_{6-\delta}$  stands out as an oxygen-deficient perovskite with a brownmillerite structure and intriguing electronic and structural features that render it an interesting subject for investigation [4]. One of the critical parameters influencing the performance of perovskite materials in practical applications is their thermal conductivity, a key factor in heat management and energy conversion efficiency.

Understanding the thermal conductivity of  $\text{CaSrFe}_2\text{O}_{6-\delta}$  is essential for optimizing its performance in various applications, yet a comprehensive exploration of this property, particularly in relation to oxygen stoichiometry, remains relatively unexplored in the literature. This study aims to bridge this gap by providing information of the thermal conductivity of  $\text{CaSrFe}_2\text{O}_{6-\delta}$ . By employing advanced experimental techniques, we seek to unravel the intricate interplay between crystal structure, oxygen vacancy, and thermal transport mechanism in this intriguing perovskite oxide.

The significance of this research extends beyond the specific material under investigation, contributing to the broader understanding of thermal transport in complex oxides. The insights gained from this study not only enhance our fundamental

knowledge of  $\text{CaSrFe}_2\text{O}_{6-\delta}$  but also offer valuable guidance for the design and development of novel materials with tailored thermal properties for applications in emerging energy technologies. Through this investigation, we aim to pave the way for the utilization of  $\text{CaSrFe}_2\text{O}_{6-\delta}$  in advanced materials for efficient heat management and energy conversion processes.

## Experiment

$\text{CaCO}_3$ ,  $\text{SrCO}_3$ , and  $\text{Fe}_2\text{O}_3$  powders were meticulously selected for the synthesis of  $\text{CaSrFe}_2\text{O}_{6-\delta}$ . The individual powders were precisely weighed and homogeneously mixed in stoichiometric proportions using an agate mortar and pestle. Subsequently, pellets were meticulously prepared from the powder blend under a pressure of 3 tons, followed by calcination at 1000 °C for 24 hours. The resulting pellets were then cooled to room temperature, reground, and repalletized. Sintering of the pellets took place at 1200 °C for 24 hours, with a constant heating rate of 100 °C/h throughout the calcination and sintering processes. To assess the crystal structure and phase purity of the synthesized material, powder X-ray diffraction (PXRD) with  $\text{Cu K}\alpha 1$  and  $\text{K}\alpha 2$  radiations was employed. Rietveld refinements of the XRD data were conducted using GSAS software [5] and the EXPGUI interface6. Microstructural studies were performed by scanning micrographs of the materials. The thermal conductivities of the materials were investigated using a Thermtest thermal conductivity meter, MP-2 with TPS-4. This method is based on the principle of the Transient

Plane Source Method, where a circular disc of diameter 13 mm/25mm and thickness of 3 mm was placed on the flat sensor of the Thermtest device, and the thermal conductivity was measured at room temperature.

## Results and Discussion

The material's crystal structure, identified as the brownmillerite type, has been previously reported [4]. In a recent X-ray diffraction experiment, the obtained results align

with the earlier findings (Figure 1). Specifically, the compound exhibits an orthorhombic structure with the  $Ibm2$  space group, depicted in (Figure 2) [4]. The structure consists of alternating layers of octahedra and tetrahedra. Within the same layer, the  $\text{FeO}_6$  octahedra share corners with other octahedra and with the tetrahedra in the layers above and below. Notably, the tetrahedral layer is comprised of chains of  $\text{FeO}_4$  tetrahedra running parallel to the octahedral layers [4].

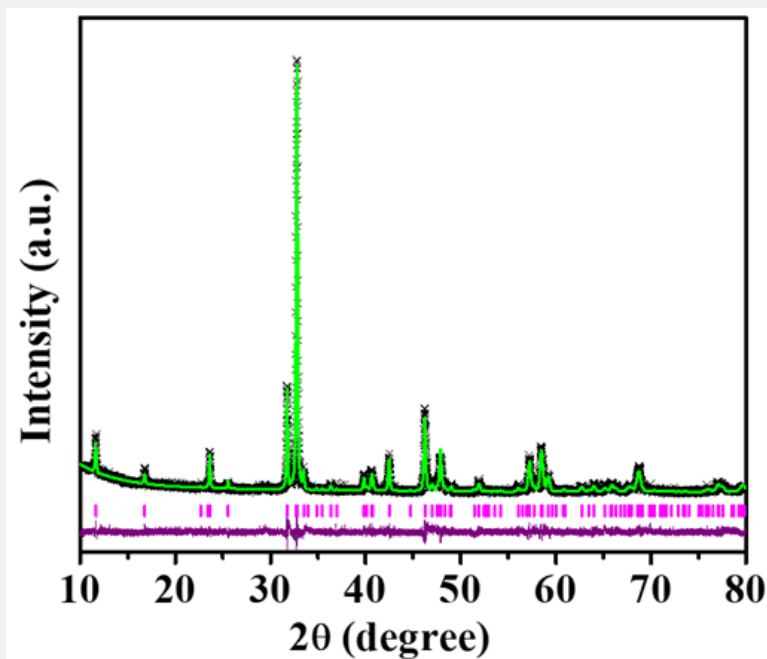


**Figure 1:** Rietveld refinement profile for powder X-ray diffraction data of  $\text{CaSrFe}_2\text{O}_{6.5}$ , space group  $Ibm2$ . Black stars, green lines, vertical pink tick marks, and lower purple lines represent the experimental data, structural model, Bragg peak positions, and difference plot, respectively.

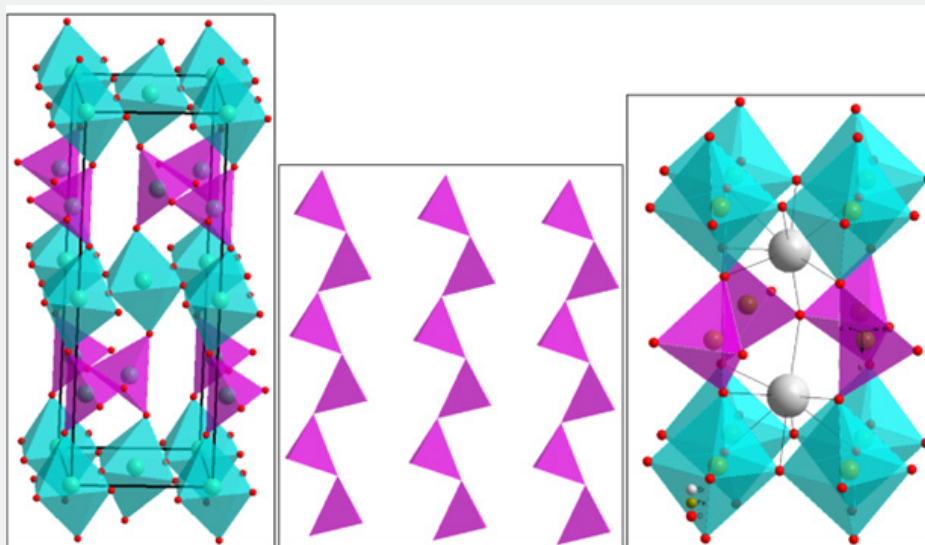


**Figure 2:** Crystal structure of  $\text{CaSrFe}_2\text{O}_{6.5}$ . (a) The octahedral  $\text{FeO}_6$  (cyan) and tetrahedral  $\text{FeO}_4$  (pink) layers. Grey spheres represent Ca/ Sr. (b) View from the top to highlight the chain formation in the tetrahedral layer. The Sr atoms are omitted for clarity. (c) Coordination geometry of Ca/Sr atoms. Note that Sr is 8-coordinated.

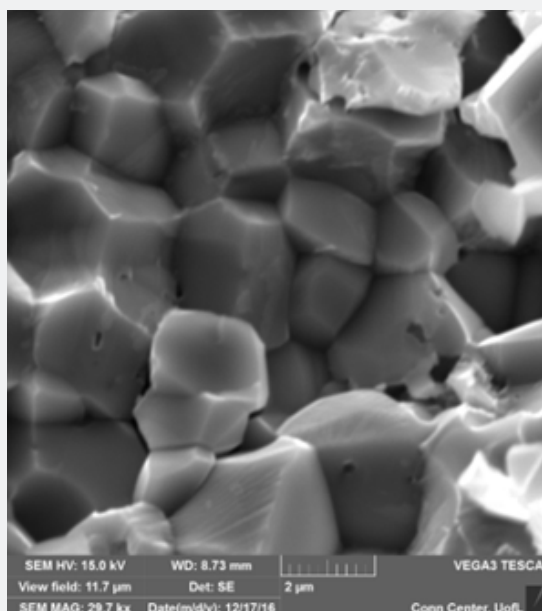
A distinctive feature of this material is the coordination number 8 observed for the A-site cations, illustrated in Figure 2c. This arrangement is characteristic of the brownmillerite-type structure. Table 1 shows the Rietveld refinement parameters for the *Ibm2* space group of  $\text{CaSrFe}_2\text{O}_{6-\delta}$ . Figure 3 shows the SEM

image for the micrograph of the crystallites of  $\text{CaSrFe}_2\text{O}_{6-\delta}$ . It is revealed from the SEM image that the crystallites grow in uniform geometry and sizes. It is nonporous and grain boundaries are formed between the crystallites.

**Table 1:** Rietveld refinement parameters of  $\text{CaSrFe}_2\text{O}_{6-\delta}$ .

element	x	y	z	Uiso	multiplicity	occupancy
Ca	0.5126(7)	0.1109(4)	0.0085(6)	0.029(8)	8	0.5
Sr	0.5126(7)	0.1109(4)	0.0085(6)	0.029(8)	8	0.5
Fe1	0.0760(2)	0.25	-0.0039(4)	0.027(4)	4	1
Fe2	0.25	0	0	0.038(6)	8	1
O1	0.2260(9)	0.0067(3)	0.2931(0)	0.028(7)	8	1
O2	-0.0815(6)	0.1490(7)	0.0016(2)	0.028(7)	8	1
O3	0.3834(3)	0.25	0.8913(3)	0.028(7)	4	1

Space group = *Ibm2*, a = 5.6315(4) Å, b = 15.1809(9) Å, c = 5.4696(8) Å, wRp = 0.0262, R<sub>p</sub> = 0.0187



**Figure 3:** SEM image of  $\text{CaSrFe}_2\text{O}_{6-\delta}$ .

### Thermal conductivity

The material shows a thermal conductivity of 0.574 W/m/K. This low thermal conductivity or high thermal insulation property of the material can be discussed based on the different factors. The thermal conductivity of materials is often influenced by the movement of electrons, with  $\text{Fe}^{3+}$  and  $\text{Fe}^{4+}$  spins potentially playing a role in this process [7]. However, thermal conductivity is a complex phenomenon, and various factors contribute to its control. In the context of electron-doped materials like  $\text{CaMnO}_3$  or  $\text{Ca}_{0.9}\text{R}_{0.1}\text{MnO}_3$ , the influence of phonon scattering becomes more pronounced, overshadowing the contributions of electrons and spins [7].

Similarly, studies on a  $\text{SrTiO}_3$ -related oxygen-deficient compound have revealed that phonon scattering has a dominant effect over electronic contributions [8]. The total thermal conductivity (K) is the sum of contributions as shown by equation 1 from phonons ( $K_p$ ) and photons (radiation)  $K_r$ .  $K_p$  includes thermal conductivity contributions from grain boundaries, lattice, and point defects [9].

$$K = K_p + K_r \quad (1)$$

As phonon scattering increases, thermal conductivity tends to decrease [10]. Heat flow occurs through a range of phonons with different wavelengths and mean-free paths, and interference on thermal phonons hinders heat propagation [11,12]. Local lattice

distortions, structures with void spaces, and random vacancies act as sites for phonon scattering, leading to reduced thermal conductivity.

In the case of our materials, the low thermal conductivity is attributed to the suppression of lattice thermal conductivity and increased phonon scattering, primarily due to the presence of oxygen vacancies [13]. This effect is consistent with previous findings that show how introducing oxygen vacancies can suppress thermal conductivity [13].

In summary, oxygen vacancies play a crucial role in enhancing phonon scattering and reducing thermal conductivity in our materials. The significance of phonon scattering, as discussed above in relation to factors such as grain size, boundaries, and spins, underscores that the presence of oxygen vacancies is a key contributor to the observed low thermal conductivity in our compound.

### Conclusion

Thermal conductivity of oxygen-deficient perovskite,  $\text{CaSrFe}_2\text{O}_{6-\delta}$  is being investigated for its thermal insulation property. It has brownmillerite-type oxygen vacancy arrangements.  $\text{CaSrFe}_2\text{O}_{6-\delta}$  shows a thermal conductivity of  $\sim 0.6 \text{ Wm}^{-1}\text{K}^{-1}$  which is one of the lower thermal conductivity of reported perovskite oxides. The main contributing factors for lowering the thermal conductivity of these compounds is phonon scattering due to oxygen vacancies and their ordered arrangements.

### Acknowledgment

This work is supported in part by the National Science Foundation Tribal College and University Program Instructional Capacity Excellence in TCUP Institutions (ICE-TI) award # 1561004. A part of this work is also supported by NSF grant no. HRD 1839895. Additional support for the work came from ND EPSCOR STEM grants for the purchase of a potentiostat and X-ray diffractometer and the American Indian College Fund for the thermal conductivity meter. The views expressed are those of the

authors and do not necessarily represent those of United Tribes Technical College.

### References

1. Wu T, Gao P (2018) Development of Perovskite-Type Materials for Thermoelectric Application. *Materials* 11(6): 999.
2. Hona RK, Huq A, Ramezanipour F (2017) Unraveling the Role of Structural Order in the Transformation of Electrical Conductivity in  $\text{Ca}_x\text{Fe}_{1-x}\text{CoO}_{6-\delta}$ ,  $\text{CaSrFeCoO}_{6-\delta}$ , and  $\text{Sr}_2\text{FeCoO}_{6-\delta}$ . *Inorg Chem* 56(23): 14494-14505.
3. Hona RK, Thapa AK, Ramezanipour F (2020) An Anode Material for Lithium-Ion Batteries Based on Oxygen-Deficient Perovskite  $\text{Sr}_2\text{Fe}_2\text{O}_{6-\delta}$ . *Chem Select* 5(19): 5706-5711.
4. Hona RK, Huq A, Mulmi S, Ramezanipour F (2017) Transformation of Structure, Electrical Conductivity, and Magnetism in  $\text{AA}'\text{Fe}_2\text{O}_{6-\delta}$ , A = Sr, Ca and A' = Sr. *Inorg Chem* 56(16): 9716-9724.
5. Larson AC, Dreele RB, Toby BH (1994) General structure analysis system - GSAS/EXPGUI, pp. 748.
6. Toby BH (2001) EXPGUI, a graphical user interface for GSAS. *J Appl Crystallogr* 34: 210-213.
7. Wang Y, Sui Y, Wang X, Su W, Liu X, et al. (2010) Thermal conductivity of electron-doped  $\text{CaMnO}_3$  perovskites: Local lattice distortions and optical phonon thermal excitation. *Acta Materialia* 58(19): 6306-6316.
8. Rahman JU, Nam WH, Van Du N, Rahman G, Rahman AU, et al. (2019) Oxygen vacancy revived phonon-glass electron-crystal in  $\text{SrTiO}_3$ . *J Eur Ceram Soc* 39(2): 358-365.
9. Schlichting KW, Padture NP, Klemens PG (2001) Thermal conductivity of dense and porous yttria-stabilized zirconia. *J Mater Sci* 36(12): 3003-3010.
10. Zhang P, Gong L, Lou Z, Xu J, Cao S, et al. (2022) Reduced lattice thermal conductivity of perovskite-type high-entropy  $(\text{Ca}_{0.25}\text{Sr}_{0.25}\text{Ba}_{0.25}\text{RE}_{0.25})\text{TiO}_3$  ceramics by phonon engineering for thermoelectric applications. *J Alloys Compd* 898: 162858.
11. Snyder GJ, Toberer ES (2008) Complex thermoelectric materials. *Nature Mater* 7(2): 105-114.
12. Maire J, Anufriev R, Yanagisawa R, Ramiere A, Volz S, et al. (2017) Heat conduction tuning by wave nature of phonons. *Sci Adv* 3(8): e1700027.
13. Hona RK, Karki SB, Dhaliwal G, Guinn M, Ramezanipour F (2022) High Thermal Insulation Properties of  $\text{A}_2\text{FeCoO}_{6-\delta}$  (A = Ca, Sr). *J Mater Chem C* 10: 12569-12573.



This work is licensed under Creative Commons Attribution 4.0 License  
DOI: [10.19080/AJOP.2024.06.555685](https://doi.org/10.19080/AJOP.2024.06.555685)

**Your next submission with Juniper Publishers  
will reach you the below assets**

- Quality Editorial service
- Swift Peer Review
- Reprints availability
- E-prints Service
- Manuscript Podcast for convenient understanding
- Global attainment for your research
- Manuscript accessibility in different formats

**( Pdf, E-pub, Full Text, Audio)**

- Unceasing customer service

**Track the below URL for one-step submission**

<https://juniperpublishers.com/online-submission.php>